

Computational Modeling and Analysis of Multiple Steady States in Vapor Compression Systems

Prashant G. Mehta

Department of Mechanical Science & Engineering,
University of Illinois,
Urbana Champaign, IL 61801
e-mail: mehtapg@uiuc.edu

Bryan A. Eisenhower

Department of Mechanical Engineering,
University of California,
Santa Barbara, CA 93106
e-mail: bryane@engineering.ucsb.edu

In this paper, we present a well-posed two-point boundary value problem framework for computing, via continuation, the steady states of interconnected vapor compression systems. We illustrate the ease and utility of our approach by employing the path following software AUTO to compute steady solutions of an experimental air-to-water heat pump that uses CO₂ as a refrigerant. We validate some of the computational solutions against the experimental data and carry out continuation and bifurcation analysis in external parameters of practical interest. The results of these computations show that multiple and qualitatively distinct distributed steady-state solutions can arise for the problem, and that our approach provides for a simpler alternative to the much harder problem of dynamic simulation. [DOI: 10.1115/1.2447237]

Keywords: heat-exchanger modeling, continuation, CO₂ refrigerant, steady-state analysis

1 Introduction

Modeling and analysis of dynamic and steady behavior of trans-critical vapor compression systems using carbon dioxide CO₂ as a refrigerant has been a focus of much recent research interest (see thesis work of Rasmussen [18], Bauer [2], Hwang [10], and Robinson [21]) because of automotive [13,8], and heating, ventilation, and air-conditioning (HVAC) [19] applications [6].

The study presented in this paper is motivated by multiple steady state behavior exhibited by an industrial vapor compression heat pump; see Sec. 2. Some of these states yield sub-par performance and are thus undesirable. Current state-of-the-art in computational modeling and analysis of these systems uses dynamic simulations; *Modelica* based libraries for components of these systems are presented in Ref. [16]. This, however, is a challenging numerical problem because of the presence of numerous interconnected nonlinear distributed and lumped elements. A typical such system consists of at least five components: axially distributed heat exchangers: (1) gas cooler, (2) evaporator, and (3) water heater elements, and lumped (4) compressor and (5) expansion valve elements (see schematic in Fig. 1). Dynamical simulations of distributed interconnected components require the numerical solution of a system of differential algebraic equations, a challenging task. A typical compromise is to either simulate a single component with appropriate boundary conditions with a high degree of accuracy [2,15] or use control-oriented reduced order modeling approaches [7,17,9] for a systems level description. The former approach is of limited relevance for the analysis of the interconnected vapor compression systems while the latter approach misses any distributed phenomena. Heat exchangers are typically long tubes that maximize the heat exchange area between two fluid paths. Analysis of distributed systems with models having only a few lumped states is approximate. Moreover, where multiple stable and unstable steady states are present, dynamic simulations will miss any unstable ones. We believe that charting out both stable and unstable steady states is important

to understanding transitions between states, as seen in the experiment.

In addition to dynamic modeling of these systems, steady-state approaches have been considered in the literature for obtaining solutions and for system optimization purposes; see the review paper of Browne-Bansal [4]. Robinson-Groll [20] obtain steady solutions for an air-air heat pump using finite elements to discretize the distributed gas cooler and evaporator elements. Yin et al. [24] consider a similar finite-element approach for evaluating capacity of a gas cooler component model. Distributed component modeling of an evaporator also appears in Bauer [2] who considers a control volume discretization. Additionally, several authors (for e.g., Bourdouxhe et al. [3], Hwang [11], White et al. [23], and references noted in Ref. [4]) have obtained steady solutions by suitable lumped approximation of distributed components. In their review paper [4] on modeling and simulation of vapor compression systems, Browne-Bansal note that “[available steady-state] models either focus on one particular component in the system or take a very simplified (or a black-box) approach for the component submodels.” The authors call for a “global approach, whereby detailed component models are linked together to develop an accurate and complete simulation model package of a vapor compression chiller.”

The computational approach presented in this paper belongs to the category of steady-state approaches, providing a complete analysis of multiple stable and unstable steady states of axially distributed vapor compression systems in a systematic manner. In contrast to the earlier approaches, we focus on the properties of the equations describing the steady model of the whole system rather than on discretization of individual system components. Suitable manipulation of the equations produces a closed two-point boundary value problem for a system of ordinary differential equations (ODEs) for which off-the-shelf continuation and bifurcation software such as AUTO [5] can be conveniently used. We construct a computational model of the experimental vapor compression system and carry out continuation and bifurcation analysis to obtain multiple distributed steady-state solutions. We validate some of these solutions with the experimental results.

The outline of this paper is as follows. In Sec. 2, we describe the experimental setup of an air-to-water heat pump that moti-

Contributed by the Design Engineering Division of ASME for publication in the JOURNAL OF COMPUTATIONAL AND NONLINEAR DYNAMICS. Manuscript received May 11, 2006; final manuscript received November 28, 2006. Review conducted by Balu Balachandran.

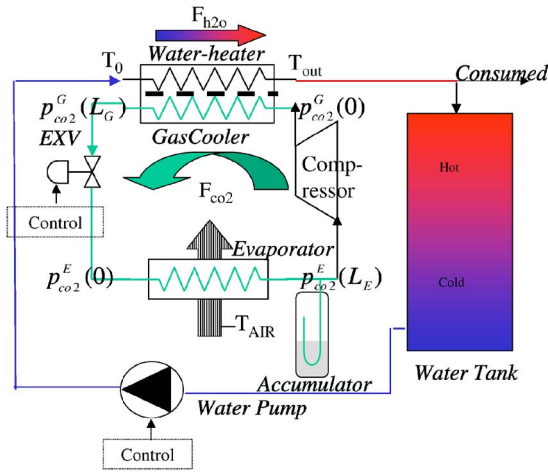


Fig. 1 Schematic representation of the experimental CO₂ air-water heat pump

valuated the modeling and computational work presented in this paper. In Sec. 3, we present a steady-state model together with a framework for computing solutions. In Sec. 4, we present the numerical results, compare these with the experiment, and use continuation to analyze the effect of parameter variations. Finally we draw some conclusions in Sec. 5.

2 Experimental Setup and Observed Behavior

Although the computational approach presented in this paper is applicable for a class of vapor compression systems, it is presented here for a particular experimental setup, for which the numerical investigation is also carried out. Figure 1 depicts the schematic of the experimental setup, an air-to-water heat pump, that uses carbon dioxide (CO₂) as a refrigerant. It consists of a gas cooler that transfers heat from CO₂ to water (whose flow rate is controlled), an expansion valve that is used to lower the pressure of the cooled gas, an evaporator that adds heat to the gas (from the surrounding ambient air), and finally an electrically operated compressor that completes the heat pump cycle. In addition, there is an accumulator at the compressor inlet which collects any CO₂ still in the liquid phase. The system is nominally operated under closed-loop control, where the water flow rate and the electronic expansion valve are controlled to track set points of output water temperature and compressor output pressure. The two main disturbances to the system are variations in the air temperature T_{AIR} and in the inlet water temperature T_0 . It is the function of feedback control to reject these disturbances.

The system of Fig. 1 is quite generic for vapor compression systems; Very similar schematics appear in Refs. [3,4,7,17,20] Having said that, details of individual experiments are almost always different: Refrigerants may be different (but works cited here all use CO₂), or details of compressor and expansion valve models may be different, or the type of heat pump application may be different (air-air or water-water heat pumps). It is not our intent here to promote up-to-date component models, a very challenging problem given the empirical nature of particularly the compressor and expansion valve models [10]. Rather, we describe a novel approach for steady-state computations that is relevant to axially distributed modeling and computations for typical interconnected vapor compression systems.

Before presenting the approach, we briefly present some of the experimental results that serve as motivation for the computational work. Closed-loop experiments with the unit show that on startup, after a brief period of transients, the system typically settles into a steady response—as determined by its sensor outputs. Figure 2 shows the cycles on the (p, h) phase diagram of the

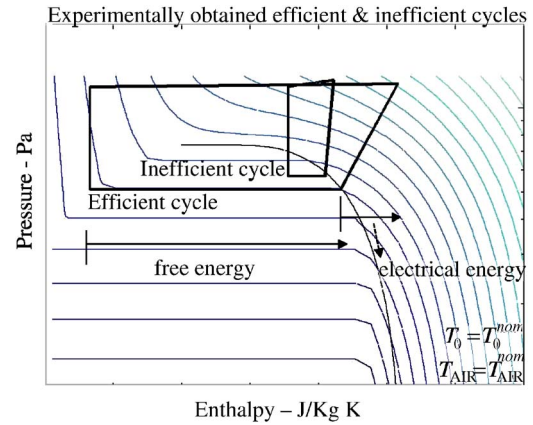


Fig. 2 Experimentally observed inefficient and efficient thermodynamic cycles (for similar nominal operating conditions). During the inefficient cycle, there is a lack of the so-called free energy absorbed from the air in evaporating the CO₂ in the evaporator.

medium. Two distinct responses are seen: (1) an efficient thermodynamic cycle; and (2) an inefficient one. Under efficient operation, the heat pump provides many units of energy to the hot water per unit of electrical energy consumed by the compressor while during the inefficient cycle, this ratio (COP) becomes close to 1. It was observed that the transition between the two cycles can be abrupt. A continuous degradation of COP as the normal ambient temperature conditions change into arctic is expected, but experimental evidence suggests that even small perturbations in operating conditions can cause the system to transition into an inefficient cycle. Figure 3(a) depicts the efficiency of the unit (COP) and Fig. 3(b) shows the temperature sensor outputs under two startup situations. In these figures, as in the remainder of this paper, we do not provide the actual numbers on the axes because of the proprietary nature of our experiment. We note, however, that the figures

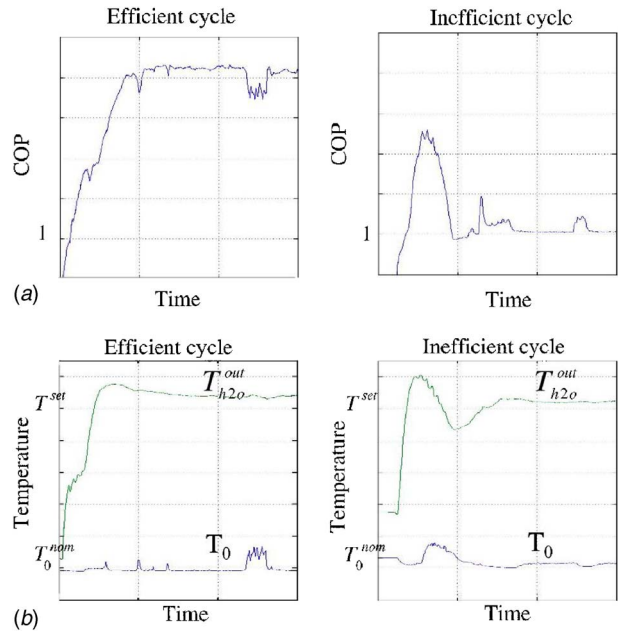


Fig. 3 Experimentally observed: (a) coefficient of performance (COP); and (b) temperature sensor outputs for the efficient and inefficient cycles during startup (T_0 denotes the inlet water temperature and T_0^{nom} is its nominal value, T_{set} is the set-point for exit water temperature T_{h2o}^{out})

depicting the CO₂ cycles will include isotherms and the saturated vapor line in the background. The figures depicting COP will indicate where its value is 1. The figures depicting air and water temperatures will indicate their nominal values. This will serve to provide qualitative comparisons. Where the comparison between experiment and numerics is given, quantitative error percentages will be provided.

There are two observations to be made regarding the experimentally observed system response: (1) the response is steady; and (2) the response shows multiple solutions. This led us to the model-based bifurcation analysis of the steady solutions of system, results of which are summarized in this paper.

3 Computational Modeling

In this section, we summarize the steady-state model equations for the experimental problem. We use a steady version of standard homogeneous equations for mass, momentum, and energy [1] together with constitutive relations for the two-phase CO₂ [14] to model the distributed gas cooler and evaporator elements and steady equations to model the lumped compressor and expansion valve. The novelty of the approach is to cast the model equations for the interconnected system as a two-point boundary value problem with constraints. In particular, we formulate the computational problem for the interconnected system as

$$\begin{aligned} \frac{d\mathbf{a}}{dx} &= \mathbf{f}(\mathbf{a}) \quad \text{for } x \in [0, 1] \\ \mathbf{g}(\mathbf{a}(0), \mathbf{a}(1)) &= 0 \end{aligned} \quad (1)$$

a two-point boundary value problem in a suitably normalized independent axial variable x . Here, the symbol \mathbf{a} denotes the vector of *states* for only the distributed components of the systems, viz., the gas cooler, the evaporator, and the water heater components. The right hand side \mathbf{f} is a suitably manipulated right hand side of the momentum and energy balance equations of these components. The steady equations of the lumped components, viz., the compressor and the expansion valve, collectively denoted $\mathbf{g}(\cdot, \cdot) = 0$, provide boundary conditions of the two-point boundary value problem (BVP). We show that the resulting problem is not well posed, in the sense that there are additional scalar unknowns. However, these unknowns are accompanied by additional constraints—that naturally arise—which provide closure to the system of equations. We further show how steady-state effects of feedback controllers present in the experiment can also be seamlessly incorporated. Each single-input–single-output (SISO) controller leads to an additional constraint together with an accompanying unknown—the control output. This results in a computationally tractable systematic approach for carrying out steady-state analysis of practical interconnected vapor compression system such as our experiment. This is important because we would like to be able to *compute* the steady solutions that have been experimentally observed. The two-point constrained BVP formulation is also convenient as off-the-shelf continuation and bifurcation software, such as AUTO [5], can then be used for carrying out detailed continuation and bifurcation analysis.

3.1 Steady Equations. We begin by modeling the distributed gas cooler and evaporator components. For CO₂, the variables of interest are density ρ , pressure p , enthalpy h , velocity u , temperature T , entropy s , and flow rate

$$F \stackrel{\text{def}}{=} \rho u A \quad (2)$$

where A is the constant cross-sectional area of the distributed element. Using this notation and homogeneous models [1], the three one-dimensional (1D) steady-state balance laws for mass, momentum, and energy are

$$\frac{\partial F}{\partial x} = 0 \quad (3)$$

$$F \frac{\partial u}{\partial x} = -A \frac{\partial p}{\partial x} - L_f F |u| \quad (4)$$

$$F \frac{\partial h}{\partial x} = -Q(x) \quad (5)$$

respectively, where the loss coefficient L_f models the pressure loss due to friction (see for e.g., [6] for semi-empirical formulae); and Q denotes the heat exchanged with the surroundings. The balance laws Eqs. (3)–(5) together with the constitutive relationships

$$\rho = \rho(p, h) \quad (6)$$

$$T = T(p, h) \quad (7)$$

$$s = s(p, h) \quad (8)$$

are used to model the gas cooler and the evaporator components. In either of these components, because of Eq. (3) and the fact that neither the compressor nor the valve store any mass we have

$$F(x) \equiv F \quad (9)$$

i.e., a constant, though not a priori known, CO₂ flow rate. We assume pressure p and enthalpy h to be *the* state variables and express the momentum and energy balance laws in these state variables as

$$\frac{\partial p}{\partial x} = - \frac{F \rho_h}{(F^2 \rho_p - A^2 \rho^2)} Q + L_f \frac{F^2 \rho}{(F^2 \rho_p - A^2 \rho^2)} \quad (10)$$

$$F \frac{\partial h}{\partial x} = -Q(x) \quad (11)$$

where Eq. (6) is obtained from substituting Eqs. (2) and (6) into Eq. (4); and ρ_p and ρ_h denote partials of the constitutive relationship Eq. (6) with respect to p and h , respectively. Such a representation, where the velocity u has been eliminated and instead replaced with (constant) flow rate F together with density ρ and its partials—dependent only upon the states via the constitutive relationship—is useful in obtaining the computational approach. The two Eqs. (10) and (11) together with the constitutive relationships and appropriate boundary conditions describe the steady-state behavior of either the gas cooler or the evaporator. For the interconnected system, the appropriate boundary conditions arise because of the compressor and the expansion valve equations.

We use the notation (p^E, h^E) for evaporator and (p^G, h^G) for gas cooler; $Q = Q^G$ for gas cooler and $Q = Q^E$ for evaporator. These variables are axially distributed and their terminal values, viz. $(p^E(L^E), h^E(L^E))$ and $(p^G(0), h^G(0))$ are input and output variables, respectively, for the compressor. Similarly, $(p^G(L^G), h^G(L^G))$ and $(p^E(0), h^E(0))$ are input and output variables, respectively, for the expansion valve; L^E and L^G denote the axial lengths of the evaporator and gas cooler, respectively. Using these terminal values, we model the mass and energy balance [17,22] for the compressor as

$$\rho^E(L^E) \omega V \eta_{\text{vol}}(r) = F \quad (12)$$

$$[h^G(0) - h^E(L^E)] \eta_{\text{isen}}(r) = [h_{\text{isen}} - h^E(L^E)] \quad (13)$$

where ω is the angular velocity of the compressor shaft; ωV is the ideal volumetric flow rate of the compressor; h_{isen} denotes the enthalpy at the compressor output if the transition from inflow to outflow in the compressor were isentropic, i.e.

$$s[p^E(L^E), h^E(L^E)] = s[p^G(0), h_{\text{isen}}] \quad (14)$$

and $\eta_{\text{vol}}(r)$, $\eta_{\text{isen}}(r)$ are (pressure ratio $r = p^G(0)/p^E(L^E)$ dependent) volumetric and isentropic compressor efficiency characteristics. The two expansion valve equations are modeled as (see for e.g., Ref. [17])

$$h^E(0) = h^G(L^G) \quad (15)$$

$$\frac{[\rho^E(0) + \rho^G(L^G)]}{2} c_A V_{\text{pos}} [p^G(L^G) - p^E(0)] = F^2 \quad (16)$$

where Eq. (15) expresses modeling assumption of isenthalpic valve and Eq. (16) is a Bernoulli equation for momentum balance; $c_A V_{\text{pos}}$ is the (discharge) valve coefficient.

We assume that water does not change its state as it is heated and model the energy exchange between the gas cooler and the water heater as

$$C_v F_{h2o} \frac{\partial T_{h2o}}{\partial x} = Q^G \quad (17)$$

where C_v denotes the water specific heat, and Q^G the heat exchanged with the gas cooler. For water, there is also a boundary condition

$$T_{h2o}(0) = T_0 \quad (18)$$

We next write an expression for heat exchanged with the surroundings for evaporator

$$Q^E(x) = A_{\text{exch}}^E \alpha^E [T_{\text{AIR}} - T^E(p, h)(x)] \quad (19)$$

and for the gas cooler

$$Q^G(x) = A_{\text{exch}}^G \alpha^G [T_{h2o}(x) - T^G(p, h)(x)] \quad (20)$$

where A_{exch}^* are the contact areas; α^* are the heat transfer coefficients; T_{AIR} is the ambient air temperature; and Eq. (7) is used to evaluate $T = T(p, h)$. The heat transfer coefficient α^G for gas cooler is assumed to be a constant while for the evaporator, where the CO_2 fluid is in two phase, $\alpha^E = \alpha^E(h)$ is modeled using an empirical relationship—the so-called modified Bennett–Chen’s relationship described in Ref. [10].

Finally, in order to obtain a consistent set of equations for the purpose of our computational approach, we make a coordinate change $x \rightarrow L^G x'$ for the gas cooler and water heater equations and $x \rightarrow L^E x'$ for the evaporator. In the normalized coordinate, we express states as $p'(x') = p(x)$ and $h'(x') = h(x)$ to obtain the modified version of the two equations of state, Eqs. (10) and (11), expressed in their functional form

$$\frac{\partial p'}{\partial x'} = f_p(p', h'; \lambda) \quad (21)$$

$$\frac{\partial h'}{\partial x'} = f_h(p', h'; \lambda) \quad (22)$$

where $\lambda \in R^n$ is a vector of external parameters. We carry out a similar normalization of the independent coordinate for Eq. (17) and denote the right hand side of the resulting equation by symbol f_T .

3.2 Boundary Value Problem. After making the coordinate change to the normalized coordinate (and dropping primes), the equations of state for the heat pump consists of five ODEs

$$\frac{\partial p^E}{\partial x} = f_p(p^E, h^E; T_{\text{AIR}}) \quad (23)$$

$$\frac{\partial h^E}{\partial x} = f_h(p^E, h^E; T_{\text{AIR}}) \quad (24)$$

$$\frac{\partial p^G}{\partial x} = f_p(p^G, h^G; T_{h2o}) \quad (25)$$

$$\frac{\partial h^G}{\partial x} = f_h(p^G, h^G; T_{h2o}) \quad (26)$$

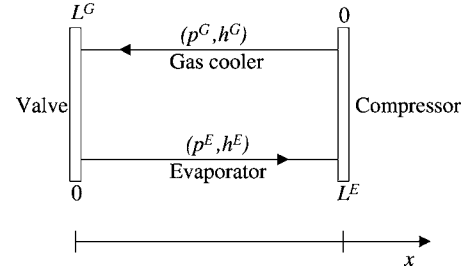


Fig. 4 Schematic representation of the two-point boundary value problem

$$\frac{\partial T_{h2o}}{\partial x} = f_T(p^G, h^G, T_{h2o}) \quad (27)$$

together with five boundary conditions, expressed in the normalized coordinate as

$$T_{h2o}(0) = T_0 \quad (28)$$

$$\rho^E(L^E) \omega V \eta_{\text{vol}} \left[\frac{p^G(0)}{p^E(1)} \right] = F \quad (29)$$

$$[h^G(0) - h^E(1)] \eta_{\text{isen}} \left[\frac{p^G(0)}{p^E(1)} \right] = [h_{\text{isen}} - h^E(1)] \quad (30)$$

$$h^E(0) = h^G(1) \quad (31)$$

$$\frac{[\rho^E(0) + \rho^G(1)]}{2} V_{\text{pos}} c_A [p^G(1) - p^E(0)] = F^2 \quad (32)$$

Figure 4 schematically depicts the above two-point boundary value problem with the independent coordinate x . For a given F and h_{isen} , the above constitutes a two-point BVP with five equations in five unknowns $\mathbf{y} = (p^E, h^E, p^G, h^G, T_{h2o})$. Since the flow rate F and h_{isen} are both unknowns, there are two additional equations

$$s[p^E(1), h^E(1)] = s[p^G(0), h_{\text{isen}}] \quad (33)$$

$$\int_0^{L^E} \rho^E(p^E, h^E)(x) dx A^E + \int_0^{L^G} \rho^G(p^G, h^G)(x) dx A^G = M_0 \quad (34)$$

that yield a closed system with unknowns $\{\mathbf{y}(x), F, h_{\text{isen}}\}$. The latter Eq. (34) expresses the mass conservation of CO_2 in the system, M_0 being the mass of CO_2 circulating in the system.

In the experiment, however, there is an accumulator that drains any liquid at the compressor inlet and the circulating amount M_0 may change with the operating condition. One approach, that we take here, to model the effect of the accumulator is that the exit of the evaporator always remain on the saturated vapor curve in the CO_2 phase diagram (see Fig. 5). Mathematically, this is accomplished by substituting Eq. (34) with

$$\sigma[p^E(1), h^E(1)] = 0 \quad (35)$$

where $\sigma(p, h)$ is the parametric representation of the saturated vapor curve. In this case, the mass of CO_2 in the system is given by Eq. (34) and may well vary as an external parameter is varied. Physically, this corresponds to the liquid mass that is lost to the accumulator as a result of the constraint Eq. (35).

3.3 Feedback Control. The computational approach also allows us to include the two feedback controllers present in the experiment as additional constraints:

1. In steady-state, the expansion valve control is

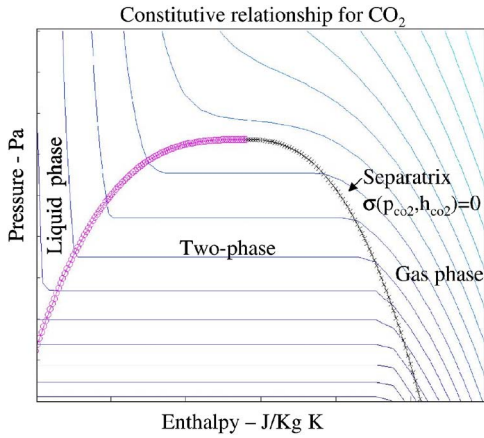


Fig. 5 Constitutive relationship for CO₂ showing isotherms and the (approximation of) saturated vapor line

$$V_{\text{pos}} = V_{\text{pos}}^0 + K_c [P^G(1) - P_{\text{set}}] \quad (36)$$

where K_c is the control gain and $V_{\text{pos}}^0, P_{\text{set}}$ are the nominal values chosen to regulate the exit compressor pressure.

- In steady state, the water flow rate control is

$$F_{h_{2o}} = F_{h_{2o}}^0 + K_T (T_{h_{2o}}^{\text{out}} - T_{\text{set}}) \quad (37)$$

where K_T is the control gain; and $F_{h_{2o}}^0, T_{\text{set}}$ are the nominal values chosen to regulate the exit water temperature $T_{h_{2o}}^{\text{out}} = T_{h_{2o}}(1)$.

The control gains are obtained by using the steady-state value for the proportional integral differential (PID) controllers used in the experimental system. Mathematically, the presence of two controllers leads to two additional Eqs. (36) and (37) and two additional unknowns $V_{\text{pos}}, F_{h_{2o}}$.

The ease with which additional equations pertaining to feedback control can be incorporated systematically into the framework illustrates the flexibility of the computational approach.

3.4 Constitutive Relationship. The constitutive relationship Eqs. (6)–(8) exists in the form of a table obtained using the software REFPROP [14]. For any given (p, h) , the values of $(T, s, \rho, \rho_p, \rho_h)$ are linearly interpolated from the table. Figure 5 depicts the isotherms together with the regions of liquid, gas, and two-phase CO₂. The saturated vapor curve separating the two phase and the gaseous regions is parametrically obtained as

$$p = 7.36 \times 10^6 \left[1 - 12.5 \left(\frac{h}{3.4 \times 10^5} - 1 \right)^{2.5} \right] \quad (38)$$

and is used to derive the constraint Eq. (35). The parametric curve approximates the saturated vapor line quite reasonably for actual operating points. At very low pressures, the approximation deteriorates but these points are not important.

3.5 Problem Parameters. Table 1 summarizes the problem parameters whose nominal values are needed. These values are obtained from physical considerations; the lengths and areas are obtained from experiments, the physical properties of CO₂ are used to derive the values of heat transfer coefficients, and experiments are used to obtain compressor efficiency characteristics. We refer the interested reader to Refs. [10,20] for discussion on selection of some of these parameters. The two parameters, inlet water temperature T_0 and air temperature T_{AIR} , are used as continuation parameters that are varied.

Table 1 Physical parameters in the CO₂ model

Component	Parameter	Description
Gas cooler	L^G	axial length
	A^G	cross-sectional area
	L_f^G	loss coefficient
	α^G	heat transfer coefficient
Evaporator	A_{exch}^G	exchange area (heat xfer)
	L^E	axial length
	A^E	cross-sectional area
	L_f^E	loss coefficient
Water heater	α^E	heat transfer coefficient
	A_{exch}^E	exchange area (heat xfer)
	L^G	axial length
	C_V	specific heat
Compressor	$F_{h_{2o}}$	water flow rate
	$T_{h_{2o}}^{\text{out}}$	exit water temperature
	ωV	ideal compressor flow rate
	η_{vol}	volumetric efficiency
Expansion valve	η_{isen}	isentropic efficiency
	$c_A V_{\text{pos}}$	valve discharge coefficient
	V_{pos}^0	nominal valve position
	P_{set}	set-point pressure
Control	$F_{h_{2o}}^0$	nominal water flow rate
	T_{set}	set-point water exit temperature
	K_c	control gain (expansion valve)
	K_T	control gain (water valve)

4 Results

In this section, we apply the computational framework to obtain results for the model-solution $\{y(x), F, h_{\text{isen}}, V_{\text{pos}}, F_{h_{2o}}\}$ for BVP Eqs. (23)–(27), boundary conditions Eqs. (28)–(32), constraints Eqs. (33) and (35), and constraints due to control Eqs. (36) and (37). We use the software package AUTO [5] to carry out computations. AUTO has the capability to continue and locate bifurcations of the solutions of constrained two-point BVPs. A well-posed BVP with as many boundary conditions as first-order ODEs is discretized in AUTO using the method of orthogonal collocation. A solution curve for the resulting square system of algebraic equations is continued in a single parameter using the method of arc-length continuation employing Newton iteration [12]. The discretized state, say y_d and the parameter λ are parametrized as $[y_d(s), \lambda(s)]$ where s denotes the arc length continuation parameter and λ is the external scalar parameter. For this purpose, an initial solution $x(0)$ for some given parameter value $\lambda(0)$ is needed for the continuation to begin.

In the examples presented below, there are four “extra” constraints relative to the number of ODEs and the parameters $(F, h_{\text{isen}}, V_{\text{pos}}, F_{h_{2o}})$ are then the four “extra” unknowns which make the discretized algebraic system closed (square). The parameterization for the arc-length continuation is then given as $[y_d(s), \lambda(s), F(s), h_{\text{isen}}(s), V_{\text{pos}}(s), F_{h_{2o}}(s)]$ where s as before denotes the arc length continuation parameter. COP defined as a ratio of useful energy to electrical energy (used to drive the compressor) is used as a solution measure.

4.1 Homotopy. Arc-length continuation requires a solution of the BVP for some initial choice of parameter value—a difficult proposition for the nonlinear constrained boundary value problem considered here. One solution that can be analytically written corresponds to the flow rate

$$F = 0 \quad (39)$$

however, at this limit the BVP is singular (coefficient of highest order term in Eq. (11) is zero). The solution thus is not useful for continuation. Any other solution with nonzero flow rate F is not easy to compute for the lossy BVP with an active compressor

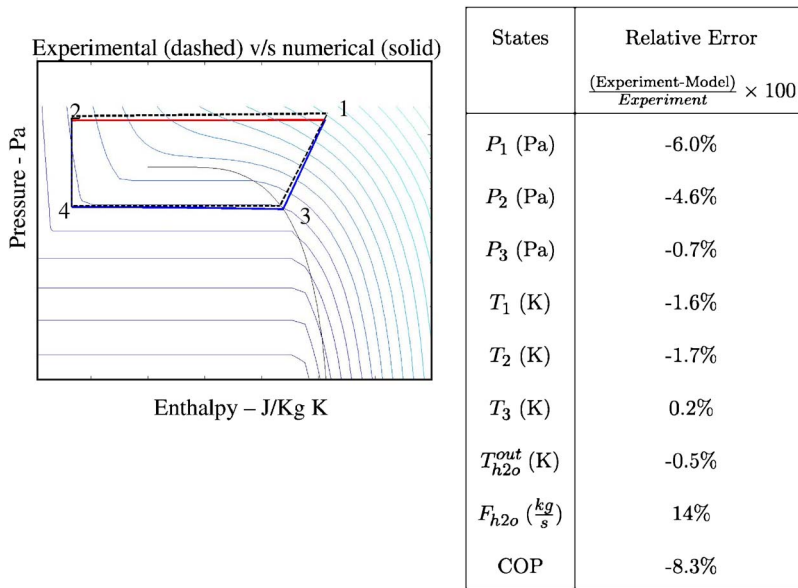


Fig. 6 The numerically obtained thermodynamic cycle and the experimentally obtained efficient cycle (for nominal values of $T_0 = T_0^{nom}$, $T_{AIR} = T_{AIR}^{nom}$). The table lists the relative errors expressed as percentage—here (P_1, T_1) are pressure, temperature sensor readings for CO_2 at Station 1 (Stations 1–4 are shown in the figure).

element. This difficulty also explains the reason for the numerical—as opposed to the analytical—nature of our investigation.

In order to obtain an initial solution point, we assume controllers are inactive and construct two homotopies to the problem:

1. **Loss homotopy** to a lossless ($L_f=0$) gas cooler and evaporator components; and a
2. **Compressor homotopy** to an idealized (but unphysical) “iso-enthalpic” compressor, where the enthalpy at the compressor output is assumed to be equal to the enthalpy of the compressor input.

Additionally, the feedback controllers are assumed to be inactive, i.e., $K_T=K_c=0$. For a lossless, iso-enthalpic compressor, we first pick a nonzero value of flow rate F and a uniform enthalpy H_0 for the initial solution, i.e.

$$h^G(x) \equiv h^E(x) \equiv H_0 \quad (40)$$

Consistent with this, we have zero heat exchange

$$\begin{aligned} Q^G(x) &\equiv 0 \\ Q^E(x) &\equiv 0 \end{aligned} \quad (41)$$

for both the gas cooler and the evaporator elements—such a solution satisfies the energy Eq. (11). For such a solution

$$p^G(x) \equiv P^G \quad (42)$$

$$p^E(x) \equiv P^E \quad (43)$$

satisfies the lossless momentum balance Eq. (10), where P^G and P^E are constants obtained by solving (using MATLAB function call *fminsearch*) the two nonlinear Eqs. (29) and (32)

$$\rho(P^E, H_0) \omega V \eta_{vol} \left(\frac{P^G}{P^E} \right) = F \quad (44)$$

$$\frac{[\rho(P^E, H_0) + \rho(P^G, H_0)]}{2} V_{posCA} (P^G - P^E) = F^2 \quad (45)$$

Finally, the values of T_0 and T_{AIR} —that provide the above solution—are obtained as

$$T_{h2o}(x) \equiv T_0 = T(P^G, H_0) \quad (46)$$

$$T_{AIR} = T(P^E, H_0) \quad (47)$$

The thermodynamic cycle corresponding to this initial solution point arises as a vertical jump on the (p, h) diagram where the pressure created by a compressor is released by a valve without any change in enthalpy.

4.2 Computations. The objectives of the computational study are to

1. Validate the model on the efficient cycle obtained in the experiment;
2. Determine, via continuation, the effect of external parameter variations (in T_{AIR} and T_0) on the system performance; and
3. Understand the experimentally observed transition from the efficient to inefficient cycle.

For the continuation study, we choose the constraint Eq. (35) which ties the inlet compressor state to the separatrix and models the effect of accumulator as discussed in Sec. 3.

We begin by obtaining the initial solution point for the homotopic limit of lossless distributed elements, iso-enthalpic compressor, and inactive controllers. Subsequently, we employ homotopic continuation to obtain a solution for the lossy system with real compressor and with the two controllers active. Next, we continue in the parameter T_{AIR} and then in the parameter T_0 to obtain the nominal solution for the external parameter values $T_{AIR} = T_{AIR}^{nom}$ and $T_0 = T_0^{nom}$ —these are the values for which experimental data exists. Figure 6 compares the cycle for the numerical solution with the experimentally obtained efficient cycle. The adjoining table tabulates the relative error between the experimental readings and the

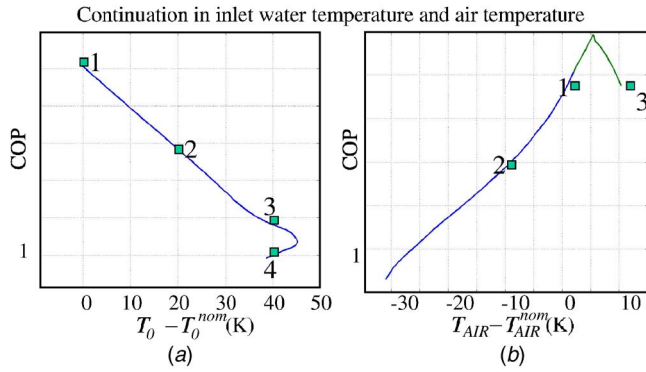


Fig. 7 COP as the solution is continued in the primary continuation parameter: (a) inlet water temperature T_0 ; and (b) air temperature T_{AIR} ; the numbers correspond to distinct cycles shown in the Fig. 8

corresponding values for the numerical solution.

We next determine the effect of variations in the two external parameters, inlet water temperature T_0 , and air temperature T_{AIR} on system performance. Figure 7 parts (a) and (b) depict the continuation diagrams as the parameters T_0 and T_{AIR} are varied. The

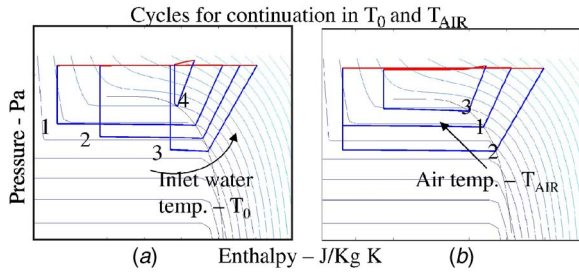


Fig. 8 Cycles as the solution is continued in the primary continuation parameter: (a) inlet water temperature T_0 ; and (b) air temperature T_{AIR}

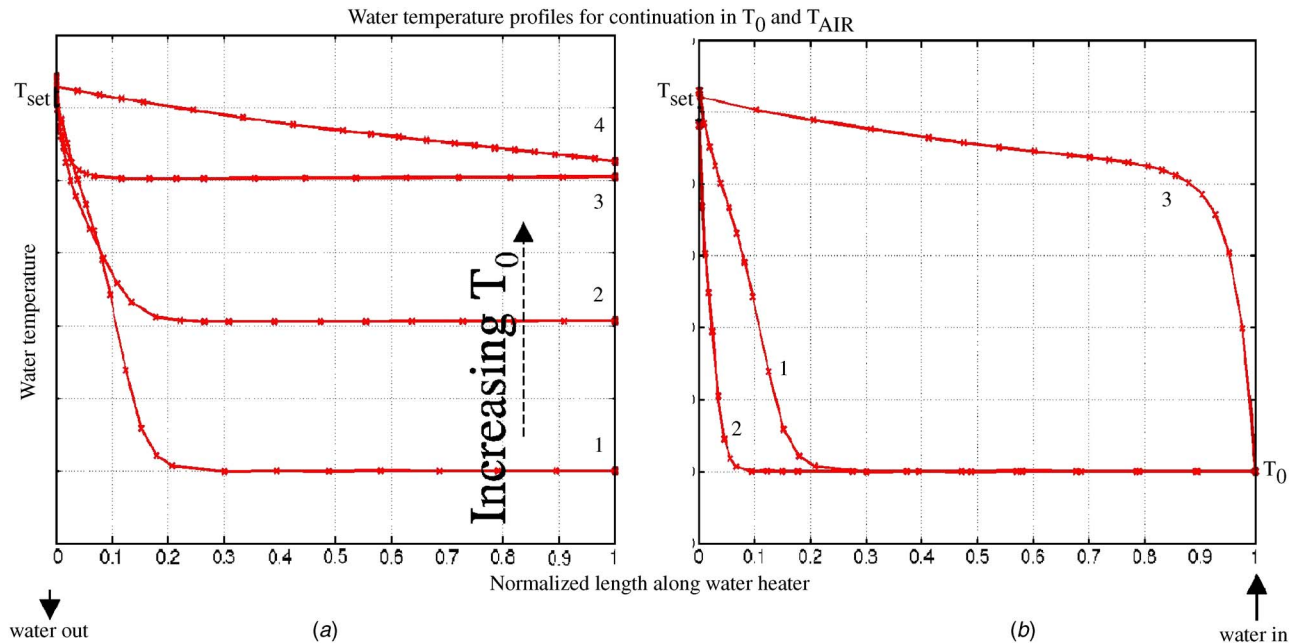


Fig. 9 Distributed profiles of water temperature $T_{h2o}(x)$ as the solution is continued in the primary continuation parameter: (a) inlet water temperature T_0 ; and (b) air temperature T_{AIR} ; “x” denotes the collocation points for discretization along the axial direction

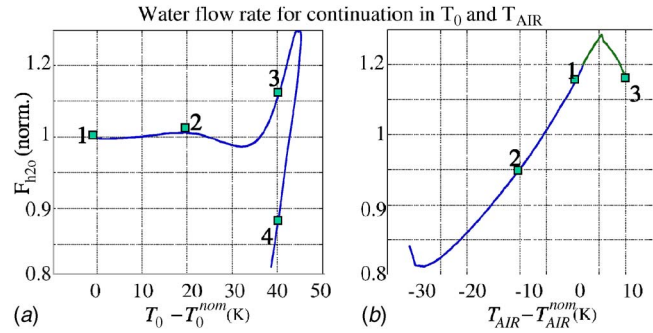


Fig. 10 Water flow rate F_{h2o} as the solution is continued in the primary continuation parameter: (a) inlet water temperature T_0 ; and (b) air temperature T_{AIR} ; the numbers correspond to distinct cycles shown in Fig. 9

cycles corresponding to the numbered solution points are shown in Fig. 8 parts (a) and (b), respectively. The number 1 always corresponds to the cycle for the nominal temperature and parameter values. This allows one to compare solutions across separate continuation diagrams.

The distributed water temperature profiles for the two continuations appear in Figure 9. The location of the collocation points is also shown in the figure, illustrating the need for adaptive gridding, used here, to resolve the longitudinal gradients whose location and size depend on the continuation parameter. Discretizations done a priori would have difficulty with convergence, particularly where the spatial profiles undergo a drastic change as fronts move from the exit of the water heater to the inlet of the water heater as in Fig. 9. We note that the feedback controller ensures that the exit water temperature is regulated at the set point T_{set} by controlling the water flow rate; see Fig. 10 for the continuation diagram of the controller water flow rate.

The continuation study shows efficient cycles with high COP values for nominal operating conditions where inlet water temperature $T_0 = T_0^{nom}$ and air temperature $T_{AIR} = T_{AIR}^{nom}$. In accordance with expectation, the COP deteriorates as either the inlet water

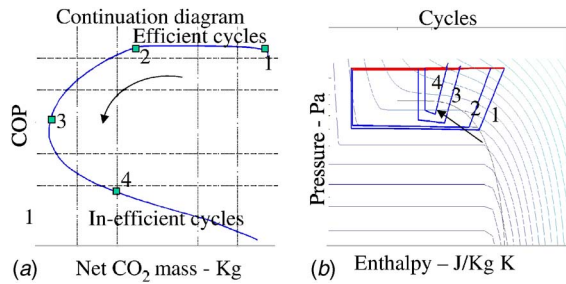


Fig. 11 (a) Bifurcation diagram obtained from varying the mass of CO₂ in the system together with (b) resulting cycles

temperature is raised (Fig. 7(a)) or the air temperature is lowered (Fig. 7(b)). We find that the heat transfer coefficient in the evaporator is a sensitive parameter that leads to *turning points* that result in multiples solutions (for e.g., solutions 3 and 4 in Fig. 7(a)). However, these solutions were found only for rather large values of inlet water temperature T_0 and not for nominal conditions as observed in the experiment.

Finally, we investigate the sensitivity of the accumulator constraint (Eq. (35)) by relaxing the constraint and allowing the inlet compressor boundary conditions to move off the separatrix. We replace the constraint in Eq. (35) with that in Eq. (34), freeze the external parameters including T_0 and T_{AIR} to their nominal values, and continue in the net mass of CO₂ in the system. Figure 11 depicts the resulting bifurcation diagram that shows a turning point in the solutions where efficient and inefficient cycles can coexist for a given net mass of CO₂ for nominal conditions. Additional analysis that can validate and explain the experimentally observed transition to inefficient cycle is a subject of ongoing investigation.

There are a couple of points to be made regarding the continuation curve in Fig. 11. One, this figure *does not* provide an explanation for the experimentally observed transition from efficient to inefficient cycle. This is because: (1) the inefficient cycles are *unstable* as the turning point leads to a change in stability type, and (2) the inefficient cycles correspond to an *unphysical* inlet compressor boundary condition. The other point is that a continuation scheme will miss any disconnected solution branches. One of our objectives in carrying out the continuation described in Fig. 11 was to possibly reach such a disconnected branch via relaxing the inlet compressor constraint. In particular, it can represent a homotopy possibly connecting two branches that are otherwise disconnected in physical space. However, two things had to happen for us to achieve our objective: (1) the compressor inlet point (on the cycle) had to move back into the saturated vapor or the gaseous phase; and (2) another turning point needed to arise while continuing the inefficient cycle portion of the branch. These are needed for the solution to be physical and stable. Neither of this occurs in Fig. 11, thereby invalidating the hypothesis. To the best of our knowledge, the inefficient cycle seen in experiments arises as a consequence of a disconnected stable solution branch that will require additional investigations.

5 Conclusions

In this paper, we presented a two-point BVP framework for computing, via continuation, steady solutions of practical interconnected vapor compressor systems. We applied the computational framework to validate the efficient cycle observed in the heat pump experiment and to determine the effect of parameter variations on system performance. The results of the computations show that multiple and qualitatively distinct distributed steady-state solutions can arise for the problem, and that our approach provides for a simpler alternative to the much harder problem of dynamic simulation.

Apart from the fact that we restrict our attention to spatially 1D equations—a reasonable assumption for many of these problems—no major simplifications are needed to carry out the steady-state analysis. Moreover, additional lumped components (for e.g., due to action of control) can be seamlessly adapted into the framework as additional constraints. The computational problem arises as a well-posed constrained two-point boundary value problem, for which off-the-shelf software packages such as AUTO [5] can most conveniently be used to compute stable as well as unstable solutions.

Although we presented our approach for the equations motivated by our experimental application, we believe it to be broadly applicable where (a) quantitatively different (from our case) compressor and expansion valve equations; or (b) other (than CO₂) refrigerants; or (c) equations with 1D-distributed as well as lumped control; or (d) some combination of the above can also be easily considered. The only limitation is that the equations of distributed elements must be 1D—a reasonable assumption for many of these problems.

Acknowledgment

Comments from an anonymous referee helped improve this paper. In particular, the discussion on stability and disconnected branches is directly as a result of these comments. The authors are grateful to Clas Jacobson for suggesting the bifurcation problem observed in the CO₂ experiments. Jesper Ooppelstrup helped with the problem definition, numerical values of the model coefficients used in the study, and provided useful comments on the paper. The authors acknowledge useful comments from Tobias Sienel and Marios Soteriou that helped improve the presentation of this paper. This work was supported in part by the United Technologies Research Center (UTRC), East Hartford, CT.

References

- [1] Aldridge, C. J., and Fowler, A. C., 1996, "Stability and Instability in Evaporating Two-Phase Flows," *Surv. Math. Ind.*, **6**, pp. 75–107.
- [2] Bauer, O., 1999, "Modelling of Two-Phase Flows with Modelica," Master's thesis, Lund Institute of Technology, Lund, Sweden.
- [3] Bourdouxhe, J. H., Grodent, M., Lebrun, J. L., Saavedra, C., and Silva, K. L., 1994, "A Toolkit for Primary HVAC System Energy Calculation—Part 2: Reciprocating Chiller Models," *ASHRAE Trans.*, **100**, pp. 774–786.
- [4] Browne, M. W., and Bansal, P. K., 1998, "Challenges in Modeling Vapor-Compression Liquid Chillers," *ASHRAE Trans.*, **104**(1), pp. 474–486.
- [5] Doedel, E. J., Champneys, T., Fairgrieve, T., Kuznetsov, Y., Sandstede, B., and Wang, X. J., 1997, *AUTO97: Continuation and Bifurcation Software for Ordinary Differential Equations (With HomCont)*, Concordia University, Montreal.
- [6] Fang, X., Bullard, C. W., and Hrnjak, P. S., 2001, "Modeling and Analysis of Gas Coolers," *ASHRAE Trans.*, **107**(1), pp. 4–13.
- [7] Fu, L., Ding, G., and Zhang, C., 2003, "Dynamic Simulation of Air-to-Water Dual-Mode Heat Pump With Screw Compressor," *Appl. Therm. Eng.*, **23**, pp. 1629–1645.
- [8] Giannavola, M. S., Murphy, R., Yin, J. M., Kim, M. H., Bullard, C. W., and Hrnjak, P. S., 2000, "Feasibility of Transcritical CO₂ Heat Pump for a Sport Utility Vehicle," *Proceedings of the IIR Gustav Lorentzen Conference on Natural Working Fluids*, West Lafayette, IN, July 25–28, pp. 115–122.
- [9] He, X., Liu, S., and Asada, H., 1997, "Modeling of Vapor Compression Cycles for Multivariable Feedback Control of HVAC Systems," *ASME J. Dyn. Syst., Meas., Control*, **119**, pp. 183–191.
- [10] Hwang, Y., 1997, "Comprehensive Investigation of Carbon Dioxide Refrigeration Cycle," Ph.D. thesis, University of Maryland, College Park, MD.
- [11] Hwang, Y., and Radermacher, R., 1998, "Theoretical Evaluation of Carbon Dioxide Refrigeration Cycle," *HVAC&R Res.*, **4**(3), pp. 245–263.
- [12] Keller, H. B., 1987, *Numerical Methods in Bifurcation Problems*, Springer, Berlin.
- [13] Lorentzen, G., and Pettersen, J., 1993, "A New Efficient and Environmentally Benign System for Car Air-Conditioning," *Int. J. Refrig.*, **16**(1), pp. 4–12.
- [14] McIiden, M. O., Gallager, J. G., Huper, M. L., and Morrison, G., 1993, "Refrigerant Properties Database: Capabilities, Limitations, and Future Directions," *Proceedings ASHRAE NIST Refrigerant Conference*, Gaithersburg, MD, pp. 59–71.
- [15] Pfaffert, T., and Schmitz, G., 2000, "Numeric Simulation of an Integrated CO₂ Cooling System," *Proceedings Modelica Workshop 2000*, Lund, Sweden, October 23–24, pp. 89–92.
- [16] Pfaffert, T., and Schmitz, G., 2004, "Modelling and Transient Simulations of CO₂ Refrigeration Systems Using Modelica," *Int. J. Refrig.*, **27**, pp. 42–52.
- [17] Rasmussen, B., Alleyne, A., Bullard, C., Hrnjak, P., and Miller, N., 2002,

- "Control-Oriented Modeling and Analysis of Automotive Transcritical AC System Dynamics," *Proc. 2002 American Control Conference*, Anchorage, AK, May 8–10, pp. 3111–3116.
- [18] Rasmussen, B. P., 2002, "Control-Oriented Modeling of Transcritical Vapor Compression Systems," Master's thesis, University of Illinois, Urbana, IL.
- [19] Rieberer, R., and Halozan, H., 1998, "CO₂ Heat Pumps in Controlled Ventilation Systems," *Proceedings of the IIR Gustav Lorentzen Conference on Natural Working Fluids*, Oslo, Norway, June 2–5.
- [20] Robinson, D., and Groll, E. A., 2000, "Theoretical Performance Comparison of CO₂ Transcritical Cycle Technology Versus HCFC-22 Technology for a Military Packaged Air Conditioner Application," *HVAC&R Res.*, **6**(4), pp. 325–348.
- [21] Robinson, D. M., 2000, "Modeling of Carbon Dioxide Base Air-to-Air Air Conditioners," Ph.D. thesis, Purdue University, West Lafayette, IN.
- [22] Thomas, P., 1999, *Simulation of Industrial Processes*, Butterworth Heinemann, London, UK.
- [23] White, S. D., Yarrall, M. G., Cleland, D. J., and Hedey, R. A., 2002, "Modeling the Performance of a Transcritical CO₂ Heat Pump for High Temperature Heating," *Int. J. Refrig.*, **25**, pp. 479–486.
- [24] Yin, J. M., Bullard, C. W., and Hrnjak, P. S., 2001, "R-744 Gas Cooler Model Development and Validation," *Int. J. Refrig.*, **24**, pp. 692–701.